Semester-Thesis

Coaxial Assemblies and Coplanar Waveguides for Microwave Signals up to 40 GHz

Presented by: Meinrad Sidler
Supervisor: Dr. Stefan Filipp
Prof. Dr. Andreas Wallraff
Quantum Device Lab
Laboratory for Solid State Physics
ETH Zurich

Zurich, December 13, 2010

ETH
Eidgenössische Technische Hochschule Zürich
Swiss Federal Institute of Technology Zurich

Abstract

Microwaves can be transmitted through coaxial cables with fixed impedance.

If the impedance is not constant 50 Ω along the entire cable assembly, parts of the incoming wave is reflected. The vulnerability to changes in the impedance is more severe for higher frequencies since the microwave signal is sensitive to changes on length scales comparable to the wavelength.

The goal of this thesis is to investigate the transmission and reflection of microwaves up to 40 GHz for different connectors. Testing several manufacturing procedures, the quality of a coaxial cable assembly is improved.

We could achieve reflection coefficients of less than -12 dB at the operation frequency of 40 GHz with SK-connectors and reflection coefficients of less than -27 dB at the operation frequency of 20 GHz with SMA-connectors.

In the second part of this thesis, the performance of different designs for a printed circuit board serving as a sample holder transmitting microwaves is investigated.

Contents

Chapter 1

Motivation

Strong coherent coupling between a quantum mechanical two level system and a harmonic oscillator is of great interest for numerous reasons. Traditionally, such interaction can be achieved in cavity QED experiments, where atoms coherently exchange single photons with the modes of the electromagnetic field in the cavity. QED experiments have the advantage of a long coherence time for atoms. The rather weak coupling leads, however, to long manipulation times. Furthermore, a large equipment to control the atoms is used which restricts the possibilities to integrate atom QED experiments into other systems.

In recent experiments it was demonstrated that it is possible to build a superconducting circuit which acts as an artificial atom and coherently couples to single microwave photons stored in an on-chip cavity. The advantages of such a device are strong interactions, leading to short operation time scales, and integration possibilities.

To combine the advantages of the two systems, hybrid systems are proposed to obtain coherent coupling between the two systems.

One approach is to use Rydberg atoms due to their large dipole moments and long lifetimes. To make the Rydberg atoms to interact with the solid state system, the resonance frequency of the latter should be the same as the transition frequency of the atom, around 50 GHz. As a consequence, it is necessary to provide cable assemblies which have good properties in this frequency regime and, therefore, to extend currently used technology working at frequencies up to 15 GHz.

Chapter 2

Impedance mismatch

An ideal microwave cable has along its entire length a constant impedance of 50 Ω. Also, all of the connectors should be impedance matched to 50 Ω. On real cables one observes disturbances in the impedance, especially in the connectors.

Without using a time gate (see Chapter 8), it is not possible to measure the reflection of a single connector with the network analyzer. However, the specifications of the reflection of microwave components are declared for a single device. The goal of this chapter is to estimate the factor between the reflection at a connector and the reflection at this connector at both ends of a cable. In this way, it is possible to measure a cable assembly with a certain connector at both ends and evaluate whether the connector's specification of the reflection were achieved.

The electromagnetic field is assumed to be transverse to the propagation direction (TEM). We can imagine a disturbance, which causes reflection, as shown in Figure 2.1. We consider three regions with different electrical permittivity ($\epsilon^i = \epsilon_0 \epsilon_r^i$, $i = 0, 1, T$) and magnetic permeability ($\mu^i = \mu_0 \mu_r^i$, $i = 0, 1, T$) where ϵ_r^i is the relative electrical permittivity and μ_r^i is the relative magnetic permeability of region i. We assume $\mu_r^i = 0$. This results in a first region with a refractive index $n_0 = \sqrt{\epsilon_r^0 \mu_r^0} = \sqrt{\epsilon_r^0}$, a region with a refractive index n_T and in between a region with refractive index n_1.

The incoming wave ($\vec{E}(\vec{r}, t)$, $\vec{H}(\vec{r}, t)$) and the reflected wave ($\vec{E}'(\vec{r}, t)$, $\vec{H}'(\vec{r}, t)$) are plane waves. As a consequence, the resulting superposition $\vec{E}_{tot}$, $\vec{H}_{tot}$ can be written as:

$$\vec{E}_{tot}(\vec{r}, t) = E(\vec{r}, t) + E'(\vec{r}, t) \tag{2.1a}$$

$$\vec{H}_{tot}(\vec{r}, t) = H(\vec{r}, t) + H'(\vec{r}, t) \tag{2.1b}$$

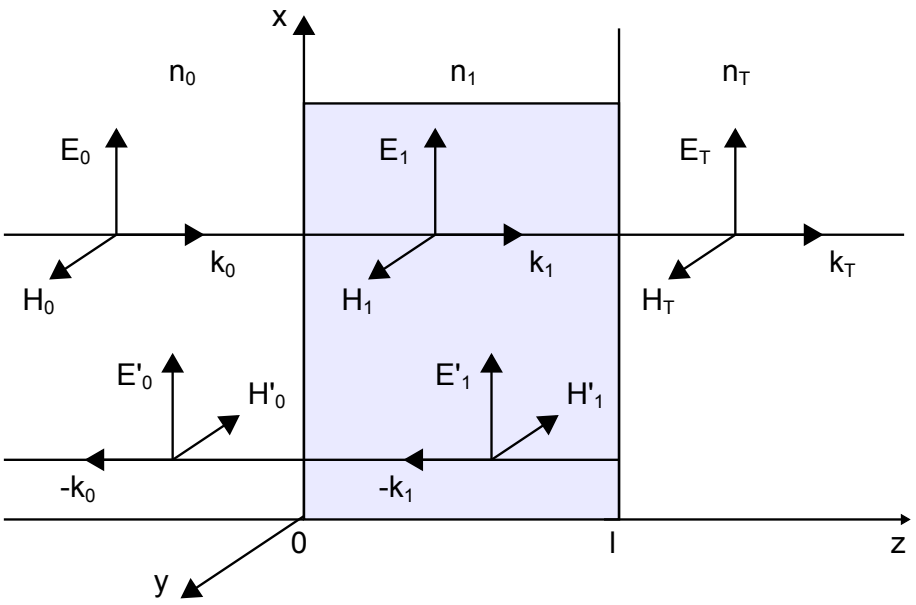

Figure 2.1: A region with different impedance.

$$\vec{E}(\vec{r},t) = \begin{cases} E_0\hat{x}e^{\imath\left(\omega t-\vec{r}\vec{k_0}\right)}, & z<0 \\ E_1\hat{x}e^{\imath\left(\omega t-\vec{r}\vec{k_1}\right)}, & 0<z<l \\ E_T\hat{x}e^{\imath\left(\omega t-(\vec{r}-l\hat{z})\vec{k_T}\right)}, & l<z \end{cases} \tag{2.2a}$$

$$\vec{E'}(\vec{r},t) = \begin{cases} E'_0\hat{x}e^{\imath\left(\omega t-\vec{r}(-\vec{k}_0)\right)}, & z<0 \\ E'_1\hat{x}e^{\imath\left(\omega t-\vec{r}(-\vec{k}_1\right)}, & 0<z<l \end{cases} \tag{2.2b}$$

$$\vec{H}(\vec{r},t) = \begin{cases} H_0\hat{y}e^{\imath\left(\omega t-\vec{r}\vec{k_0}\right)}, & z<0 \\ H_1\hat{y}e^{\imath\left(\omega t-\vec{r}\vec{k_1}\right)}, & 0<z<l \\ H_T\hat{y}e^{\imath\left(\omega t-(\vec{r}-l\hat{z})\vec{k_T}\right)}, & l<z \end{cases} \tag{2.2c}$$

$$\vec{H'}(\vec{r},t) = \begin{cases} H'_0(-\hat{y})e^{\imath\left(\omega t-\vec{r}(-\vec{k}_0)\right)}, & z<0 \\ H'_1(-\hat{y})e^{\imath\left(\omega t-\vec{r}(-\vec{k}_1\right)}, & 0<z<L \end{cases}, \tag{2.2d}$$

where $\vec{k_i}$ is the propagation vector and $\omega = \frac{c}{n_i}\left|\vec{k_i}\right|$ $(i = 0, 1, T)$ is the angular frequency of the wave. The unity vectors in x-, y- and z direction are denoted $\hat{x}$, $\hat{y}$ and $\hat{z}$. Of course, the physical field is the real part $\Re\vec{E}$ respectively $\Re\vec{H}$. We assumed a linear polarised wave.

From Maxwell's equations it holds $(i = 0, 1, T)$:

$$|E_i/H_i| = \sqrt{\frac{\mu_0}{\epsilon_0}\frac{1}{\epsilon}} \equiv \frac{\sqrt{\eta_0}}{n_i}. \tag{2.3}$$

The impedance η_0 is the vacuum impedance. We assume the absence of surface charges and -currents. As a consequence, the Maxwell equations imply that the components of the E field and the H field parallel to the surface and the

components of the D field ($\vec{D} = \epsilon\vec{E}$) and the B field ($\vec{B} = \mu\vec{H}$) perpendicular to the surface have to be continuous at the interfaces (see [2]). This leads to four boundary conditions:

A the first interface we find:

$$E_0 + E_0' = E_1 + E_1' \tag{2.4a}$$
$$H_0 - H_0' = H_1 - H_1'. \tag{2.4b}$$

Using Equation (2.3), Equation (2.4b) can be transformed into:

$$\Rightarrow n_0(E_0 - E_0') = n_1(E_1 - E_1') \tag{2.5}$$

.

For the second interface we find (again using Equation (2.3)):

$$E_1 e^{\imath k_1 l} + E_1' e^{-\imath k_1 l} = E_T \tag{2.6a}$$
$$n_1(E_1 e^{\imath k_1 l} - E_1' e^{\imath k_1 l}) = n_T E_T. \tag{2.6b}$$

We introduce the variables r for the reflection and t for the transmission:

$$r = \frac{E_0'}{E_0} \tag{2.7}$$

$$t = \frac{E_T}{E_0}. \tag{2.8}$$

We find that the boundary conditions lead to the equation:

$$\begin{pmatrix} 1 \\ n_1 \end{pmatrix} + \begin{pmatrix} 1 \\ -n_1 \end{pmatrix} r = M \begin{pmatrix} 1 \\ n_T \end{pmatrix} t. \tag{2.9}$$

Where M is the matrix:

$$M = \begin{pmatrix} A & B \\ C & D \end{pmatrix} = \begin{pmatrix} \cos(k_1 l) & -\frac{i}{n_1}\sin(k_1 l) \\ -in_1 \sin(k_1 l) & \cos(k_1 l) \end{pmatrix}. \tag{2.10}$$

The Equation (2.9) has the solution:

$$r = \frac{n_0(A + Bn_T) - C - Dn_T}{n_0(A + Bn_T) + C + Dn_T}, \tag{2.11}$$
$$t = \frac{2n_0}{An_0 + Bn_0 n_T + C + Dn_T}. \tag{2.12}$$

A difference in the refractive index $n_i = \sqrt{\epsilon_r^i}$ results in a difference in the impedance $\eta = \sqrt{\mu_i/\epsilon_i}$, $i = 0, 1, T$.

We are now interested in the difference between the following situations: In the set-up described in Figure 2.2(a) a cable has a refractive index n_0 with just one region of length l_1 with a slightly different refractive index n_1. In contrast to that, in the set-up shown in Figure 2.2(b) the cable is divided in two areas, with exactly the same properties (length l_1, refractive index n_0 as in set-up 2.2(a), which are separated by a distance l_2. The latter of the two situation is a model

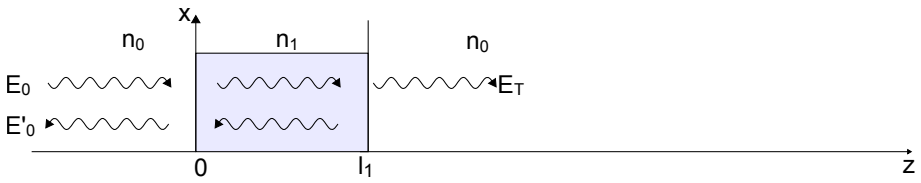

(a) One connector.

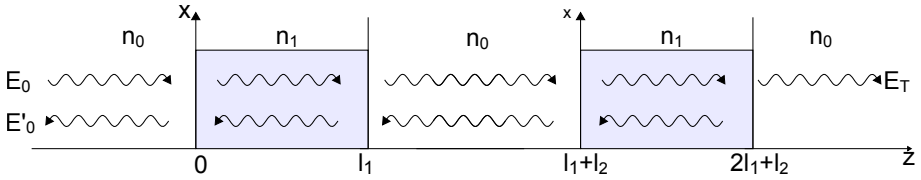

(b) Two connectors.

Figure 2.2: A sketch of the approximation of a cable as a medium with two regions (connectors) with a different impedance.

for a cable of length l_2 with plugs of length l_1. If the reflectivity of a cable is measured with a network analyzer, the total assembly is probed. In contrast, if the specifications of a single component, e.g. a plug, have to be measured, one has to check whether an assembly is as good as the plug is specified, one has to know how much higher the reflectivity of two plugs is than the one of just a single plug.

For the situation of two plugs, the matrix $M = M_a \cdot M_b \cdot M_a$ is the product of three matrices.

$$M_a = \begin{pmatrix} \cos(k_1 l_1) & -\frac{i}{n_1}\sin(k_1 l_1) \\ -in_1 \sin(k_1 l_1) & \cos(k_1 l_1) \end{pmatrix}, \; M_b = \begin{pmatrix} \cos(k_1 l_2) & -\frac{i}{n_0}\sin(k_1 l_2) \\ -in_0 \sin(k_1 l_2) & \cos(k_1 l_2) \end{pmatrix}. \tag{2.13}$$

Figure 2.3(a) shows the absolute value of $|S11_1| \equiv |r|$ for one (red, dashed line) and for two plugs ($|S11_2|$ blue), respectively. The plugs in this example have a length of 1 cm and are separated by a distance of 11 cm. The plug has a refractive index which is 25 % higher than the refractive index of the cable. Figure 2.3(b) shows exactly the same as Figure 2.3(a) but in units of dB.

The reflectivity $|S11_2|$ of two plugs clearly has an envelope function. The maxiumum of both, the envelope as well as the $|S11_1|$ is at $k_1 = N\frac{\pi}{2l_1}$ where $N \in \mathbb{N}$. However, the $|S11_2|$ is oscillating. We find that $|S11_2|$ at $k_1 = N\frac{\pi}{2l_1}$ is equal to the envelope function, if the ratio between the lengths $\frac{l_1}{l_2}$ is odd. In this way, we find the maxima M_1 for $|S11_2|$ and M_2 for the envelope function of $|S11_2|$ without analytically calculating the expression of the envelope. In Figure 2.3(a) two arrows indicate M_1 and M_2. We find the values:

$$M_1 = \left| S11_1 \left(k_1 = N\frac{\pi}{2l_1} \right) \right| = \left| \frac{n_0^2 - n_1^2}{n_0^2 + n_1^2} \right| \tag{2.14}$$

$$M_2 = \left| S11_2 \left(k_1 = N\frac{\pi}{2l_1} \right) \right| = \left| \frac{n_0^4 - n_1^4}{n_0^4 + n_1^4} \right|. \tag{2.15}$$

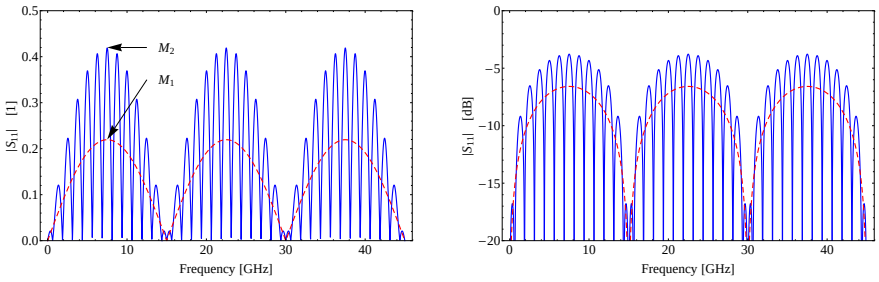

(a) Linear scale.

(b) Decibel scale.

Figure 2.3: Simulated reflection from one (red, dashed) respectively two (blue) plugs. The maximum M_2 of the envelope function of $|S11_2|$ and the maximum M_1 of $|S11_1|$ is indicated with an arrow.

Figure 2.4 shows M_1 and M_2 in dependence of the ratio $\frac{n_1}{n_0}$.

One is now especially interested in M_2/M_1 in dB units. Figure 2.5 shows this in dependency of n_1/n_0.

In the end, we don't know about the refractive index mismatch. What we do know from the measurement is the reflectivity of two plugs. What we are interested in is the corresponding reflectivity of a single connector as a function of the maximum reflection for two connectors. Practically, this means how much one can subtract on a logarithmic plot to have an idea of how much one plug would reflect. This is shown in Figure 2.6: On the x-axis the maximum of the envelope of the reflectivity of one plug is shown. On the y-axis, the ratio between one and two plugs is plotted.

Conclusively, in the regime around -20 dB, the reflectivity of two identical plugs has an envelope which is about 3 dB above the reflectivity one would measure from one single plug. This means, if a plug has a specified maximum reflectivity of -20 dB, which is the typically specified reflectivity of a MW connector, due to interference within the two plugs, the test cable can have a reflectivity of only up to -17 dB.

The power transmission in this model is the difference from the incoming wave power and the reflected wave power since we have neither taken into account the effect of the absorbing dielectric nor the resistance of the inner- and the outer conductor. However, $S12 \equiv t$ is not the ratio between the power but between the voltages. It can be calculated analogously $S11$ using formula 2.12.

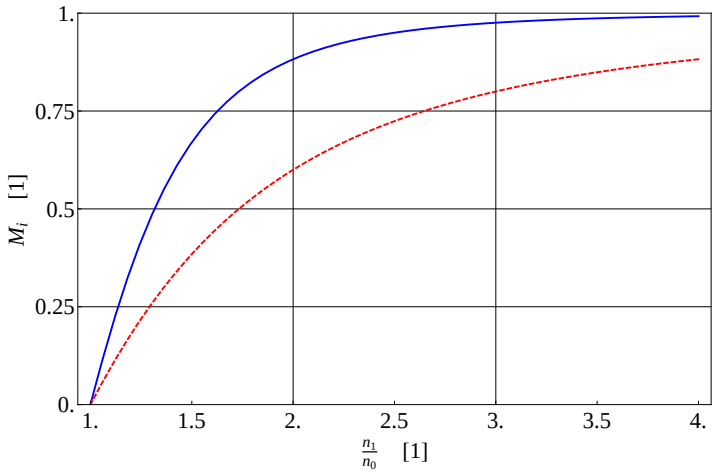

Figure 2.4: Simulated maximum reflection from one (M_1, red, dashed) respectively two (M_2, blue) plugs in dependency of $\frac{n_1}{n_0}$.

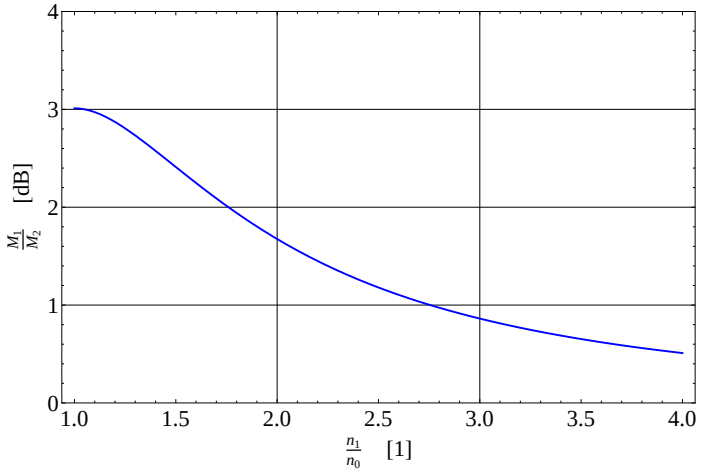

Figure 2.5: The ratio between simulated maximum reflection from one respectively two plugs in dependency of the ratio $\frac{n_1}{n_0}$.

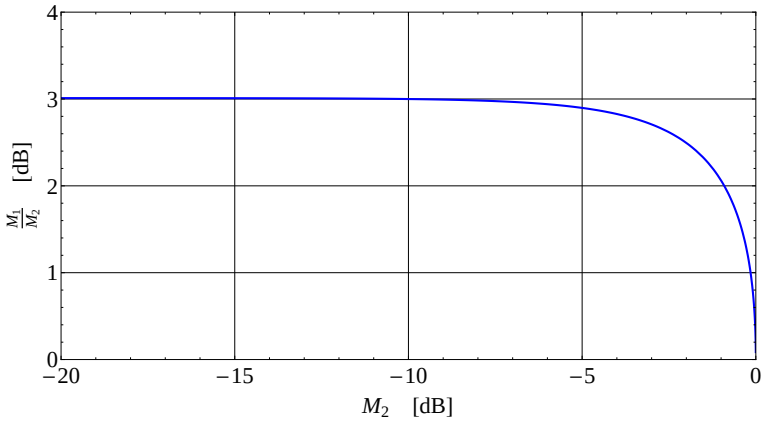

Figure 2.6: The ratio between simulated maximum reflection from one respectively two plugs in dependency of the maximum reflection from two plugs.

Chapter 3

Coaxial cables

3.1 What is a coaxial cable

A coaxial cable consists of an inner conductor with a diameter d surrounded by a dielectric which is enclosed in an outer conductor with inner radius D (see Figure 3.1(a)). It is used to transmit AC-signals. In contrast to a DC conductor, a high frequency conductor is best described by lumped elements instead of a resistance. Figure 3.1(b) shows the lumped elements of a cable with resistance R_O and inductance L_O for the outer conductor and analogously for the inner conductor. Between the two conductors there is a capacitance C and a conductance G. The circuit can be simplified by describing the outer conductor as ideal and the inner conductor with a resistance R' and an inductance L' (see Figure 3.1(c)).

In this model, we find an impedance $Z = U/I$.

$$Z = \sqrt{\frac{R' + 2\pi\nu L'}{G' + 2\pi\nu C'}}, \tag{3.1}$$

where ν is the frequency of the alternating current.
For frequencies $\nu > 1$ MHz, this can be approximated as

$$Z = \sqrt{\frac{L'}{C'}}, \tag{3.2}$$

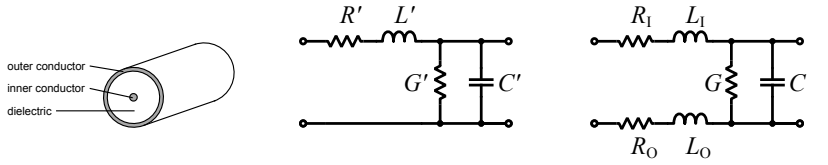

(a) Structure of a coaxial cable.

(b) Description of a coaxial cable wtih lumped elements.

(c) Simplified lumped elements circuit.

Figure 3.1: Structure and lumped elements circuits of coaxial cables.

which is independent of the frequency. For cables which are used in our experiments, the impedance is by standardization 50 Ω.

As shown in Chapter 2.3, an impedance mismatch within the cable assembly causes reflections. This is measured with a vector network analyzer (VNA). The latter has two ports which emit and measure microwaves. It measures the ratio between the voltage of the outgoing wave at port i and the voltage of the incoming wave at port j and what phase difference is in between the emitted and the measured wave. These, frequency dependent, parameters are called S_{ij}. For instance, S_{12} is the ratio between the voltage of the wave which is emitted at port 1 and the voltage of the incoming wave that is measured at port 2 and thus a parameter for the transmission. Furthermore, S_{11} is therefore a parameter for the reflection. The S-parameters are usually declared in Decibels (dB).

Apart from reflection, one is of course also interested in the transmission. At microwave frequencies, most of the deviation from unity transmission is due to reflection. However, also the resistance of inner- and outer conductor (the resistance of the inner conductor has the bigger influence than the one of the outer conductor) and, especially for frequencies over 10 GHz, the dielectric cause absorption.

3.2 Composition of coaxial cables

For testing a specific connector and in situations with no temperature gradient along the cable, we use Micro-Coax UT-085-TP semi rigid coaxial cables. The outer conductor is made of copper and plated with tin. Due to the tin-plating, it is easy to solder compared to stainless steel. Since most of the current is in the shell of the inner conductor, the latter is made of copper and has a shell of silver, which has a lower resistance than copper . Teflon (PTFE) is used as a dielectric and has a relative permittivity $\epsilon_r = 2.03$. With an inner conductor diameter $d = 0.5205$ mm and an outer conductor diameter $D = 2.2$ mm this results in an impedance $Z = 50\ \Omega$. The transmission of these cables is 100.3 dB/100 ft at a frequency of 20 GHz.

Good electrical conductivity also implies a good thermal conductivity. Thus, to transmit a signal from room temperature into the cryostat, a copper cable implies a substantial heat load for the latter. As a consequence, a stainless steel outer conductor (UT-085-SS, 211.4 dB/100 ft at 20 GHz), or even stainless steel outer- and center conductor (UT-085SS-SS, 576.4 dB/100 ft at 20 GHz) is a good compromise.

The cables that were made for the tests mentioned in this report are all made with a UT-085-TP cable.

3.3 Microwave cable connectors

AEP 9401-1583-010

For frequencies up to 20 GHz, it is best to use AEP connectors. They can easily be soldered onto the cable since they have a captive contact between the pin and the center conductor which means that one only has to solder at the transition from connector to cable. On the other hand reflections below -27 dB at 20 GHz can be achieved. The measurement results for the cable saAEP with

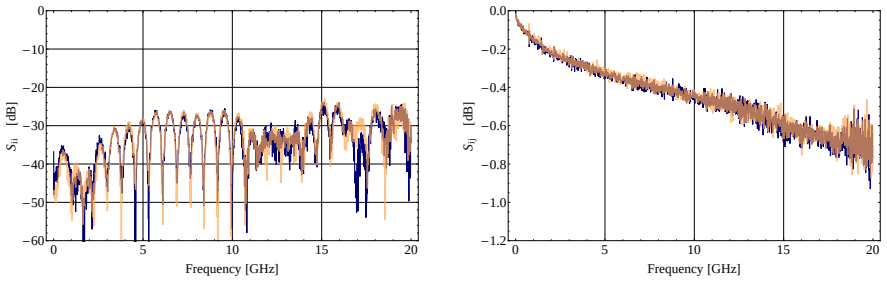

Figure 3.2: Results of cable saAEP with AEP plugs. Dark blue: S11 respectively S12, light orange: S22 respectively S21. Please notice that the scale is different from the other plots.

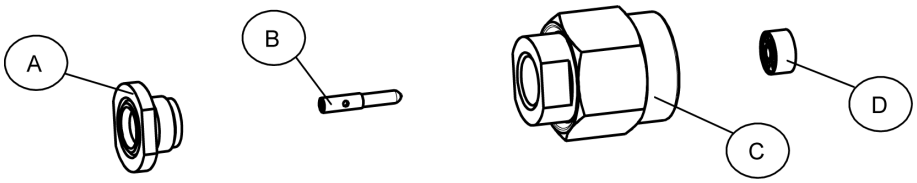

Figure 3.3: Exploded view of a Huber & Suhner 11_SK-50-2-56 plug. A is soldered on the cable. B: pin, C: ferrule, D: dielectric.

AEP connectors are shown in Figure 3.2 (S11 and S12 are represented by the dark blue curve, S22 and S21 are represented by the light orange curve).

SK male

For frequencies hihger than 20 GHz, AEP plugs are no longer suitable. Huber & Suhner have a series of connectors called SK which can be used for frequencies up to 40 GHz.

The SK plug we use in our set-ups is Huber & Suhner 11_SK-50-2-56. The return loss of this connector for the frequency range from 0-40 GHz is specified to be smaller than -20 dB.

Figure 3.3 shows an exploded view of the SK plug.

A step-by-step guide to soldering SK plugs can be found in Chapter 4.

SK female

The female counterpart to Huber & Suhner 11_SK-50-2-56 is Huber & Suhner 21_SK-50-2-58. It is specified to have a reflection of less than -21 dB for frequencies up to 40 GHz. Figure 3.4 shows the exploded view of this jack. Notice that only ferrule B needs to be soldered to the cable. Body D has a captive contact to the center conductor and is screwed onto nipple A.

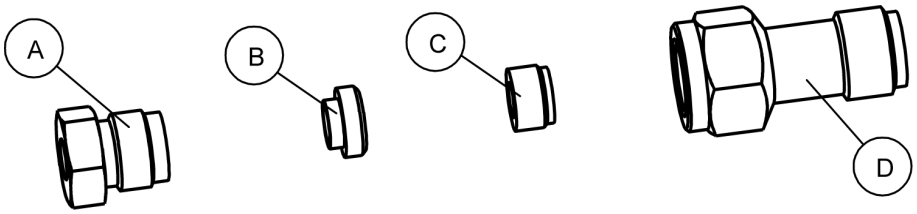

Figure 3.4: Exploded view of a Huber & Suhner 21_SK-50-2-58 jack.

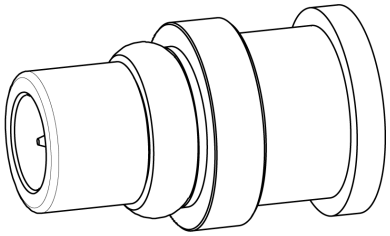

Figure 3.5: Blueprint of a Huber & Suhner 11_MMPX-50-2-1 plug.

MMPX male

To connect to printed circuit boards, MMPX connectors are used. MMPX is very small and no wrenches are needed to connect them. Furthermore, the specified maximum reflection is lower than -25 dB for frequencies up to 65 GHz which is much better than any of the connectors mentioned above. Figure 3.5 shows the blueprint of a male MMPX connector of the type Huber & Suhner 11_MMPX-50-2-1. This plug only consists of two pieces: The pin is soldered to the center conductor and the ferrule to the outer conductor.

MMPX female

The counterpart on the printed circuit board is a Huber & Suhner 92_MMPX-S50-0-1 jack (Figure 3.6). The reflection of this connector is specified to be lower than -20 dB for frequencies up to 65 GHz and lower than -22 dB for frequencies up to 26.5 GHz. More details about this connector can be found in Chapter 9.

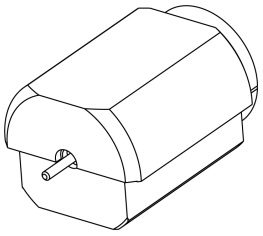

Figure 3.6: Blueprint of a Huber & Suhner 92_MMPX-S50-0-1 jack.

Chapter 4

Soldering SK-plugs

This chapter provides a step-by-step guide to soldering SK plugs. All lengths are in millimeters.

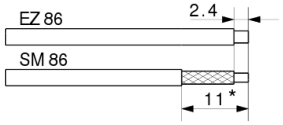

Cut the cable at the right length, strip off the outer conductor. If the cutting layer is not perpendicular to the cable, or in an other way not very well defined, it may be appropriate to shorten the cable a bit and begin again.

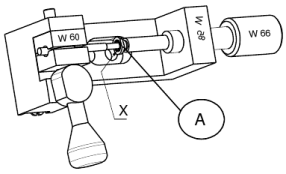

Piece A is soldered on the cable using tool W62. For this purpose, one cleans the cable with isopropyl alcohol and applies flux. It may be helpful to put the cable in a perpendicular position so that the tin can flow downwards and fill the space between the ferrule and the outer conductor.

The next step is to cut the dielectric. It is recommended to wait a day so that the dielectric can contract. To cut the dielectric, take a scalpel, push it into the dielectric without touching the center conductor, turn the cable a bit, push the scalpel again into the dielectric and focus on the ending and the beginning of the cut falling together. The result is one sharp cut. With pliers one tries to turn the dielectric. In that way, the dielectric is removed from the cable. Next, one uses sandpaper to remove the brows from the center conductor. Afterwards one cleans the latter with isopropyl alcohol to remove the metal powder.

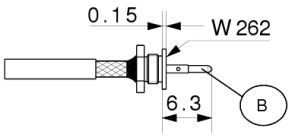

Put the pin into the corresponding tool. Place a small bit of tin wire into the pin, heat it with a small piece of aluminium foil between the pin and the soldering tip. It will take a while until the tin melts. Apply some flux onto the center conductor. Solder some tin on it. Afterwards, put the cable into the soldering fixture in such a way that the cable will slip into the pin as soon as the tin is liquid again. Hold the solder gauge in the left hand and heat the tin in the pin with the same technique as described before. When the cable slips down, make sure by moving it a bit that the tin is equally distributed. Cool the cable with isopropyl alcohol .

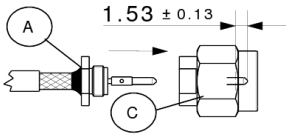

Next, screw the ferrule C on. This has to be done with a torque of 2.5 Nm. The dimensions have to be checked.

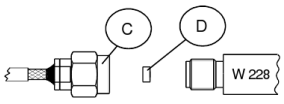

As a last step, slide insulator D carefully over center pin B and press it into connector C using the insertion tool W52.

Chapter 5

The dielectric

5.1 Cutting the dielectric

It seems to me that this is the most important step in the production of a cable assembly. The best way to cut the dielectric is by a sharp scalpel. It is best to place the scalpel as close to the outer conductor as possible, push it a bit into the dielectric, and turn the cable.

However, if one cuts too deep, the center conductor is damaged. This is shown in Figure 5.1(a): Since the skin depth of such high microwave frequencies is only very small and so the current is basically only transported by the silver layer, this is results in a highly increased reflection of up to 9 dB, see Figure 5.2(a).

On the other hand, if one cuts too shallow, the edge of the dielectric is fuzzy. Since the impedance of the plug depends on a sharp transition between pin and dielectric. An example of a badly cut dielectric is shown in Figure 5.1(b) (results in Figure 5.2(b)).

A possible way to get properly shaped edges is to cut the dielectric relatively shallow, dive it into liquid nitrogen and break it with pliers. The results are clean, sharp edges (Figure 5.1(c)). However, liquid nitrogen has its disadvantages, too, as it will be discussed in Section 5.3.

The best way to cut the dielectric is to place the scalpel on the edge of the dielectric, push it into it, turn the cable, constantly pushing it again in the dielectric and focus on ending again in the beginning of the track. Next, grab the dielectric with the pliers and turn it. One develops a feeling for whether or not the dielectric is going to tear or not. If it won't, one should make the cut more deep. The resulting edges are fulfilling the demands, which are a properly shaped edge at the transition from dielectric to the pin and no scratches in the inner conductor (Figure 5.1(d), results in Figure 5.2(c)).

5.2 Temperature dependent expansion and contraction

A further challenge is the fact that the dielectric expands when heated during soldering and afterwards contracts again. This process is slow (in the range of

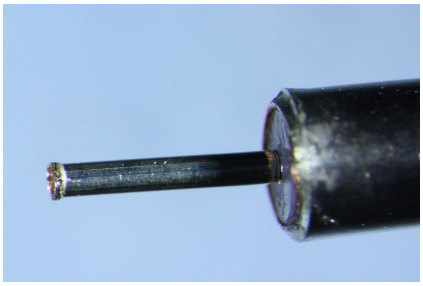

(a) Scratch in the center conductor. (Cable 13 port 2)

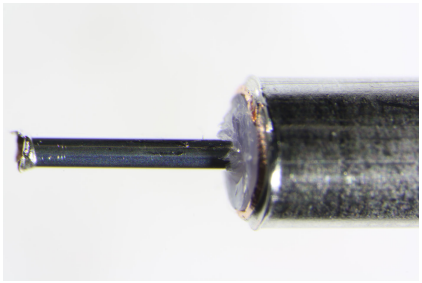

(b) Fuzzy dielectric. (Cable 9 port 1)

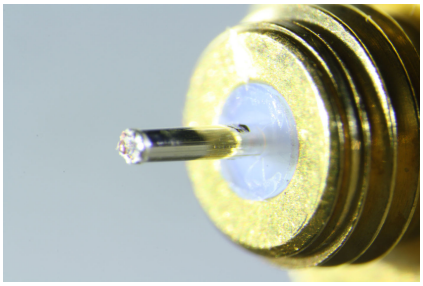

(c) Dipped in liquid Nitrogen. (Cable 7 port 1)

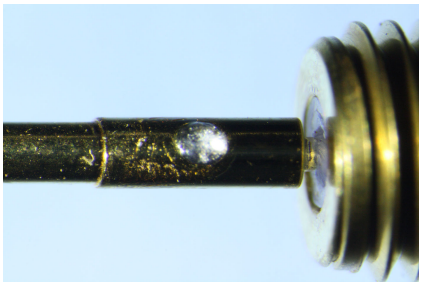

(d) Turned with the pliers. (Cable 11 port 1)

Figure 5.1: Different techniques for removing the dielectric.

hours, up to a day or two). It is unpredictable how much the dielectric will expand or contract, as a consequence, it is wise to avoid excessive heat when soldering the ferrule onto the outer conductor.

A countermeasure is to change the order of processes. It is possible to apply some tin to the outer conductor right after having removed the first 2.4 mm of the outer conductor and before cutting the dielectric. In this way, one can prevent the dielectric to expand when soldering on the ferrule. However, this procedure is only relevant for SMA plugs. In the case of SK, one cuts the dielectric after having soldered the ferrule to the outer conductor. Figure 5.3(a) shows how much the dielectric expands when applying tin. Figure 5.3(b) shows a contracted dielectric after two hours.

Figure 5.3(b) shows that it is wise to wait for approximately a day after soldering until one cuts the dielectric.

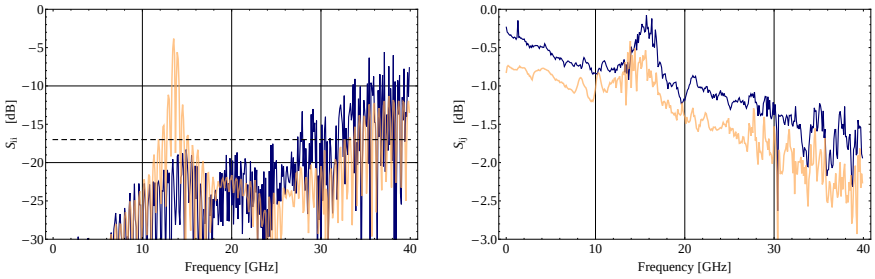

(a) Results of cable 13 (scratch in the conductor).

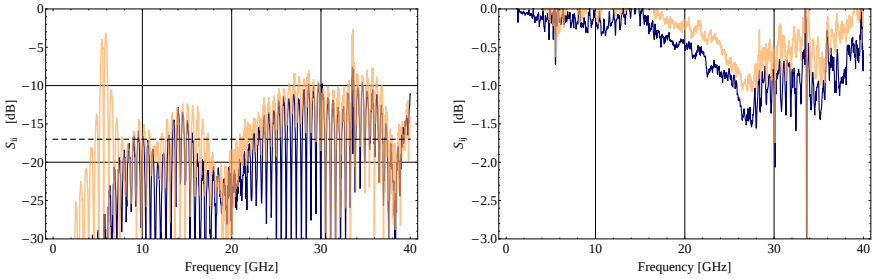

(b) Results of cable 9 (fuzzy dielectric).

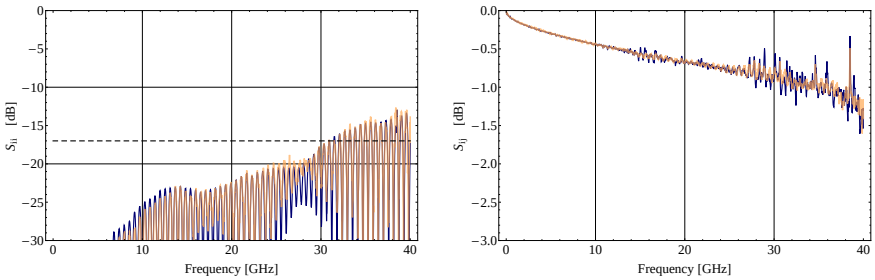

(c) Results of cable 11 (example of a properly shaped transition from dielectric to pin and no scratches in conductor).

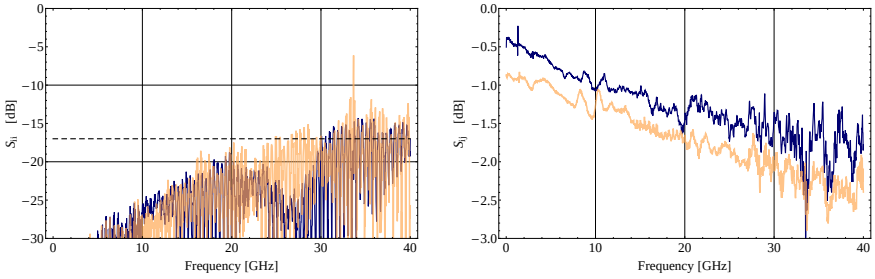

(d) Results of cable 14.

Figure 5.2: Results of different cable assemblies. Dark blue: S11 respectively S12, light orange: S22 respectively S21. The black, dashed line corresponds to the specified maximum reflection.

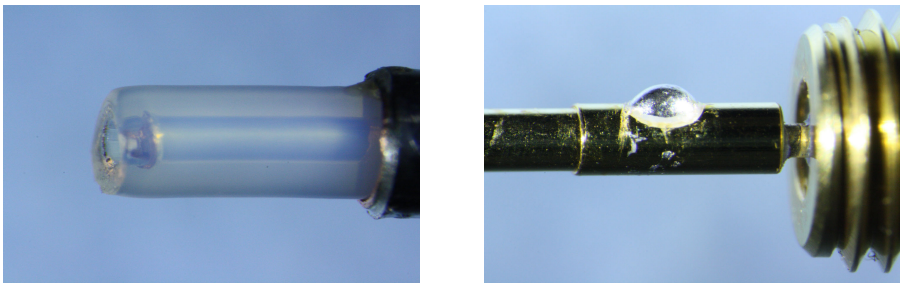

(a) Expanded dielectric (Cable 13). (b) Contracted dielectric (Cable 14).

Figure 5.3: Dielectric affected by heat during soldering.

5.3 Tensions in the dielectric

A possible explanation for the varying amount of expansion could be that there are internal tensions in the dielectric. In this case it might be helpful to get rid of these before soldering. An attempt to do this was by using liquid nitrogen. The idea is that during contraction of the dielectric it separates from the outer conductor. However, it was not possible to measure any effect of dipping the cables into liquid nitrogen before soldering.

Furthermore, this procedure also has its dangers: If there is space between the dielectric and the outer conductor, it might fill with condensated water after pulling the cable out of the liquid nitrogen. Water, as a strongly dipolar liquid, would modify the impedance.

Chapter 6

The pin

6.1 Brows

Especially when assembling cables with AEP plugs, it is important to remove the brows, since there is no tin connecting inner conductor and pin. Figure 6.1(a) (results for this cable after removal of the brows in Figure 6.2) and Figure 6.1(b) (results in Figure 5.2(b)) show a center conductor before and after removing the brows. With SMA- and SK-plugs it seems to be less important to remove brows.

6.2 Brazing solder

It is important that there is no solder on the outer surface of the center pin. I tried four methods to achieve this.

1. Apply some tin on the center conductor (using flux). Put the center conductor on when the tin is already solid. In the center pin there is a hole. I tried to touch the inner conductor through this hole with a very sharp soldering tip. However, it turns out that this method leaves a thin film of solder around the hole.

2. Keeping the soldering tin liquid while putting the center conductor on may

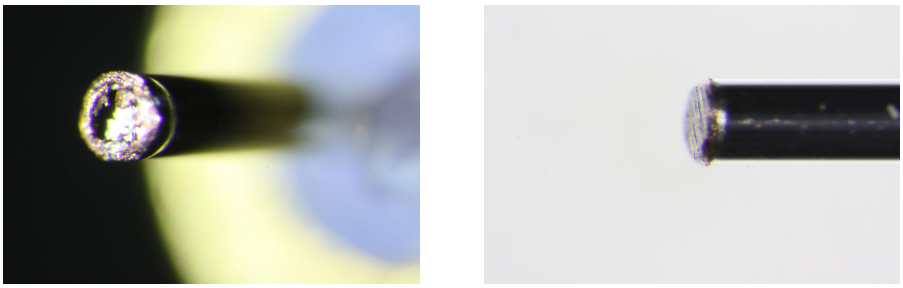

(a) Center conductor with brows (Cable 8). (b) After using sandpaper (Cable 9).

Figure 6.1: Brows.

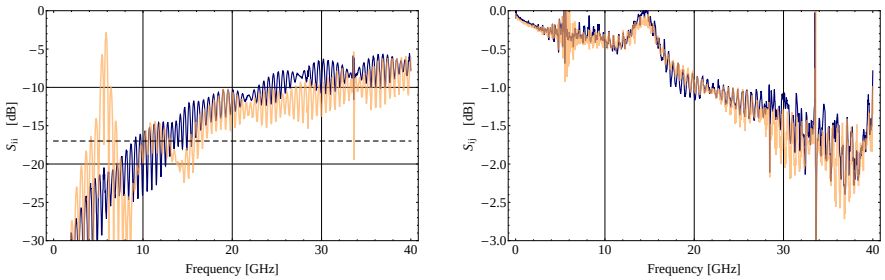

Figure 6.2: Results of cable 8. The black, dashed line corresponds to the specified maximum reflection.

leave a drop of tin at the edge of the center pin. This method was used to solder cable 9. A picture of this connector is shown in Figure 6.3(a) (results in 5.2(b)).

3. Prepare the pin by putting a small, thin piece of tin inside and melt it by touching the center pin with a small piece of aluminium foil preventing direct contact between pin and soldering tip. As a second step, when the tin is solid, put the center conductor loose into the pin and melt the tin inside the pin again with the same method. The cable now "drops" into the pin. Still, some of the tin escapes through the hole in the pin. However, it can be cut with a scalpel. Figure 6.3(b) shows a picture of cable 8 where the pin was directly touched with the soldering tip. The residues are clearly visible (results in Figure 6.2). For cable 11 (Figure 6.3(c)) a piece of aluminium foil was used (results in Figure 5.2(c)).

4. Same as the third method but melting the tin wire inside the pin by using the heat gun. I enlarged a hole of a broken sample holder to fix the center pin. However, in this way, there are residues of the sample holder on the pin.

5. Furthermore, with a resistance soldering systems, it is possible to solder more precisely. The step of attaching the pin on the inner conductor can easily be performed as follows: A small piece of a very thin wire of tin is put into the pin, the latter is squeezed between the two electrodes. The current lets the tin melt and it is possible to push the pin on the center conductor. In this way, almost no tin residue will be left on the outside of the pin.

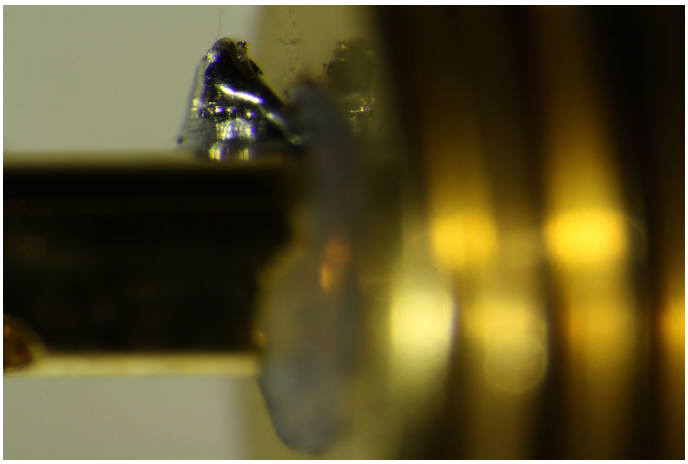

(a) A drop of tin at the edge of the pin (Cable 9).

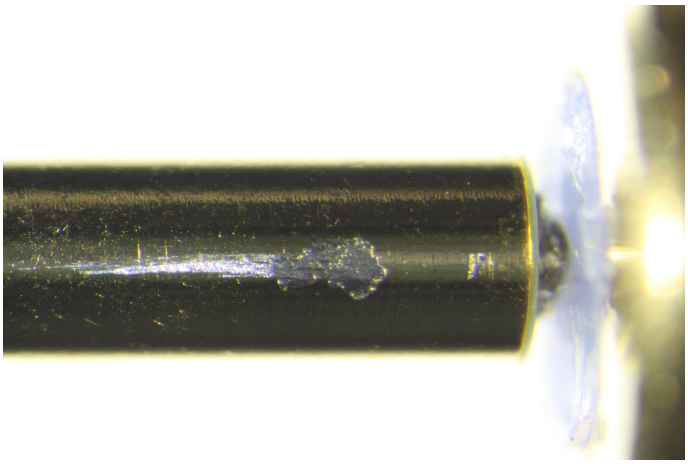

(b) The residue of the soldering tip (Cable 8).

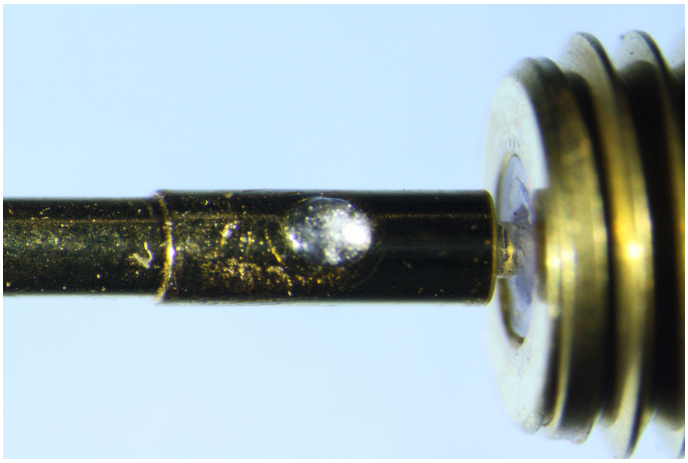

(c) A drop escaping through the hole in the pin (Cable 11).

Figure 6.3: Tin residues.

6.3 Summary

The following table summarizes the features of some cables which are discussed in the last chapters.

Cable number	Keywords	Maximum of S11
Cable 8	Residues on the pin because it was directly touched with the soldering tip	-5 dB
Cable 9	Fuzzy dielectric, drop of tin at the hole in the pin	-7 dB
Cable 11	Example of a properly shaped transition between dielectric and pin, no scratches in center conductor. For this cable the center pin was soldered on to the center conductor using an aluminium foil to prevent from contact with the soldering tip.	-13 dB

Chapter 7

Soldering connectors

In conclusion, there are several critical steps when soldering a plug.

1. The dielectric
   (a) has to be sharply cut.
   (b) has to be cut at an exact locatian relative to other parts.
   (c) must not be subject to tensions.
2. The center conductor
   (a) must not be scratched.
   (b) must be freed from brows.
3. The pin
   (a) should have full contact with the center conductor.
   (b) should not be covered with tin.
4. The ferrule
   (a) should have full contact to the outer conductor.

Chapter 8

Outlook

A very useful feature of vector network analyzers, which I have not yet used for the cables in the time when this work was done but which has successfully been tested afterwards, is the time gate. By Fourier transform, the device can switch into the time domain. It is then possible to see where the incoming wave is scattered and, as a second step, one can define a time gate covering just this impurity and switch back to frequency domain to measure the frequency dependence of the S-parameters of the selected time gate. By using this method, it is possible to check whether the specified quality can be reached. For more details about time-domain measurement see Ref. [3].

Chapter 9

Sample holder

9.1 Introduction

The chip is placed on a printed circuit board (PCB) sample holder that provides the interface to the signal generators respectively the measurement instruments. It consists of an Arlon AD 1000 substrate with a dielectric constant of $\epsilon_r = 10$ between two gold-coated layers. At the narrow side of the sample holder (for blueprints see Figure 9.1) Huber & Suhner MMPX connectors are attached and in the middle there is a cut-out in which the chip is placed. Coplanar waveguides (CPWG) on the top layer connect the MMPX connector to the chip. The chip is connected to the coplanar waveguides via bridges. To test the performance of such a sample holder, a few examples without chips are produced. The design, the attachment of the connector and the measurement results will be presented in the next sections.

9.2 Design

The PCB consists of an Arlon substrate (AD 1000). The length and width of the PCB are chosen to fit in between the electrodes forming the atom trap. The width of the inner conductor $W = 100$ µm and the gap $\rho = 160$ µm between inner- and outer conductor can be calculated from the thickness of the substrate and its permittivity $\epsilon_r = 10$.

The design of the footprint, which is the area where the connector is soldered onto the board, was calculated using computer simulations by Huber & Suhner. Figure 9.1 shows the blueprints of different board designs for testing purposes.

The general coplanar waveguide design consists of a metallized layer on the bottom, the substrate in the middle, an inner conductor surrounded by two outer conductor on the top layer (see [5]). To make sure that the outer conductors are properly grounded, it is recommended to drill vias, metal coated holes through all three layers to form an electrical connection between top and bottom layer. In the blueprints, the vias are drawn in blue. The most general test device is a PCB with just one straight line on it. This is realized in sample E on the blueprints. Figure 9.2 show an example of such a sample holder.

In addition, to see the influence of the length of the coplanar waveguide, a slightly shorter PCB was produced. This corresponds to G in the blueprints.

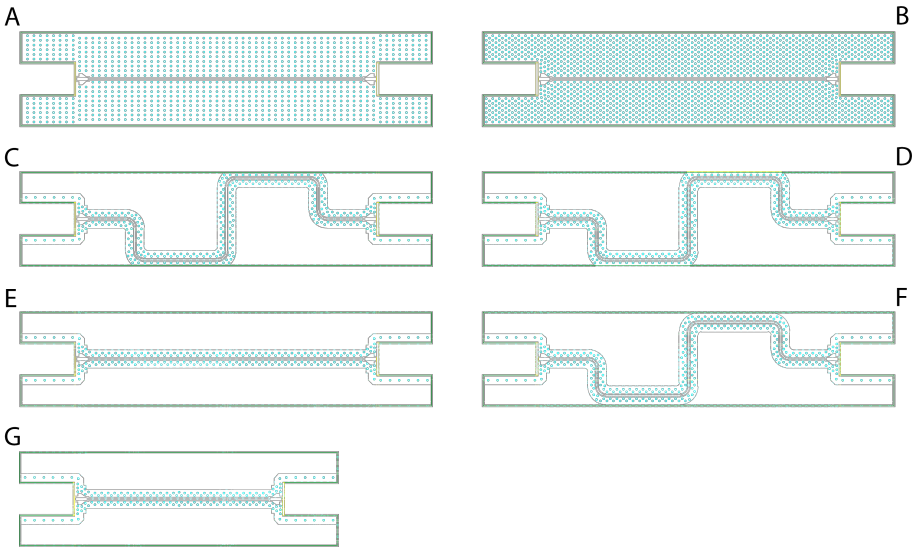

Figure 9.1: Blueprints of different versions of the sample holder's PCB.

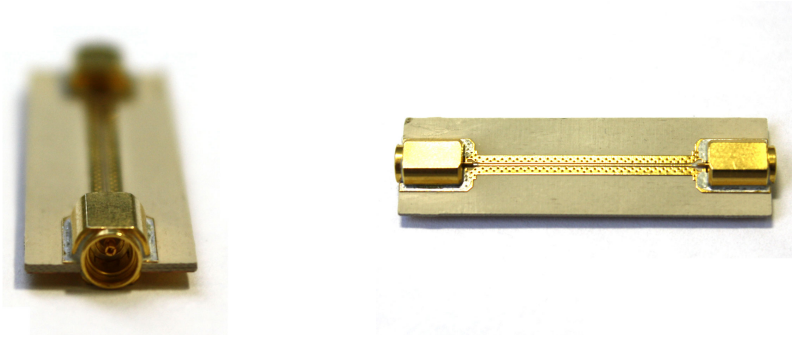

(a) Front view (b) Top view

Figure 9.2: A straight coplanar waveguide between two MMPX connectors.

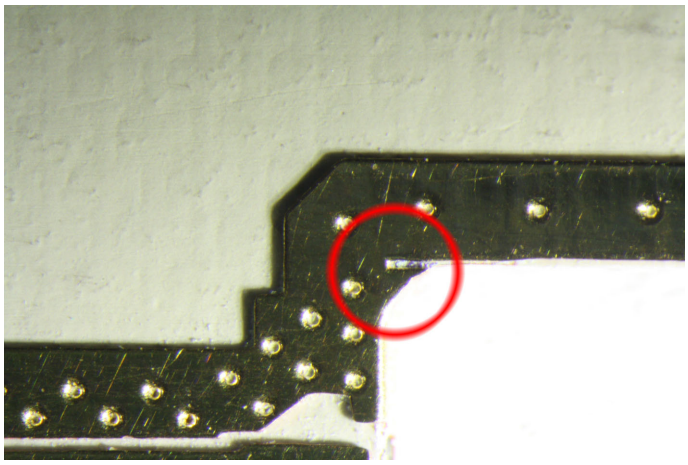

Figure 9.3: The cut-out for the MMPX plug is not as flat as it should be.

A further variation are curves. In the final design, due to the orientation of the sample, curves will be necessary. However, each curve will also reflect. For the curves, three test PCB are designed: Model F would be a good choice because the outer conductors have a width which is higher than the distance between the two outer connectors. Furthermore, the density of vias is as high as the restrictions from the manufacturing allow. However, due to the fact that the width of the sample holder is limited and the length of the sample should be as large as possible, it might be necessary to move the coplanar waveguide closer to the edge of the board as shown in model C. One thought was to compensate the lack of vias in this design by an edge metallization. This was realized in design D (edge metallization is indicated in yellow).

In the final design, the whole upper layer, except for the gap next to the inner conductor, will be metallized in order to prevent ionization of the substrate which would disturb the trajectory of the Rydberg atoms. This is realized in model A. To check the influence of the density of vias, model B with more vias was designed, too.

9.3 Mounting the MMPX plug

For the connector there is a gap at the narrow edge of the PCB. Figure 9.5 shows a section drawing the MMPX plug mounted on the PCB.

The difficulty is to put the right amount of solder paste at the right places. If its to much solder paste, the risk of a short is bigger, if it is too little, the contact between the front of the connector and the edge-metallization of the PCB is not good enough resulting in a high reflectivity. It turned out that the PCB can't be used out of the box because the milling radius is finite and results in a gap between the front of the plug and the edge-metallization. Figure 9.3 shows an example of a round corner. Possible solutions to solve this problem is to cut the corners with a scalpel or to sandpaper a bezel into the connector.

In the long term, a solution might be to enlarge the cut-out with a circle in the edge to be sure that there is no curvature in the corner of the gap

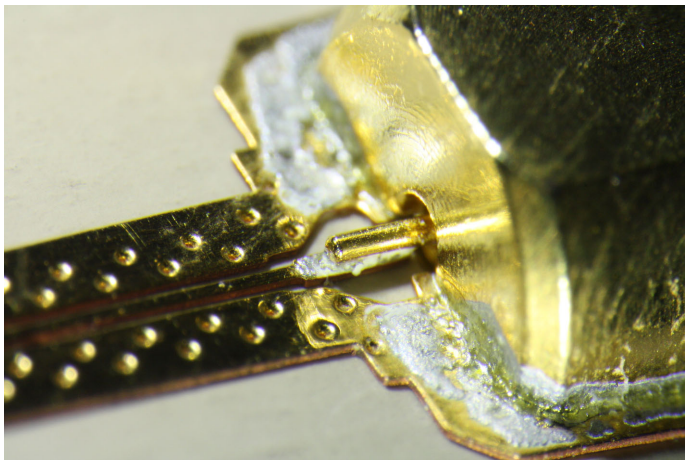

Figure 9.4: MMPX connector soldered onto the PCB.

preventing the connector to be inserted correctly. Figure 9.4 shows the connector inserted into the gap with a good contact. On the other hand, one also sees the disadvantages of the solder paste: the tin is not distributed very well defined and it may easily happen that the device is shortened.

9.4 Measurement results

The reflectivity (S21) of one plug according to a simulation should be as shown in Figure 9.6.

To measure the reflectivity of one plug and not of the whole PCB, one can do a time-domain measurement. It is possible to make such a measurement with a vector network analyzer. The latter can either be operated in band- or in low-pass mode. Furthermore, one can either measure the impulse- or the step response. For our purposes, a band-pass step measurement is adequate.

Measurement of a short, straight PCB (design G)

The goal we want to achieve is a reflection of less than -10 dB for frequencies up to 40 GHz which is possible, according to the simulation done by Huber & Suhner.

The first attempts of soldering a PCB resulted in shortened contacts.

The first measurement results are from M190410, a short sample holder (design G). Figure 9.7(b) shows the time-domain results of the first plug indicating the different gates used in Figure 9.7(a). The frequency domain measurements in Figure 9.7(a) are consequently just for one plug. Figure 9.8 shows the same for the second plug.

The PCB M190410 has an impedance which is too deep (the level of the real part of S11 is lower than the one from the matched cables. This is the result from a transition to a higher impedance). In contrast, the impedance of the fully metallized PCB M310510FM is too high. Furthermore it is clearly visible that the first connector of M190410 is better than the second one. For both

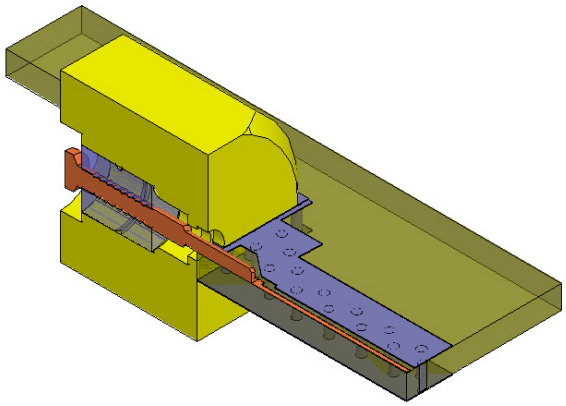

Figure 9.5: Section drawing of the MMPX connector inserted in the cut-out of the PCB.

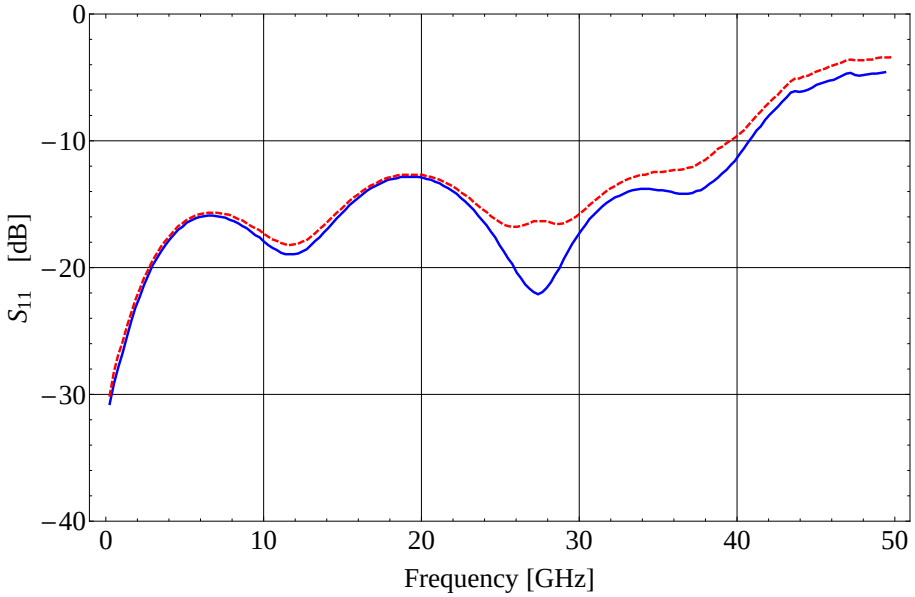

Figure 9.6: Simulations of the reflectivity (S21)

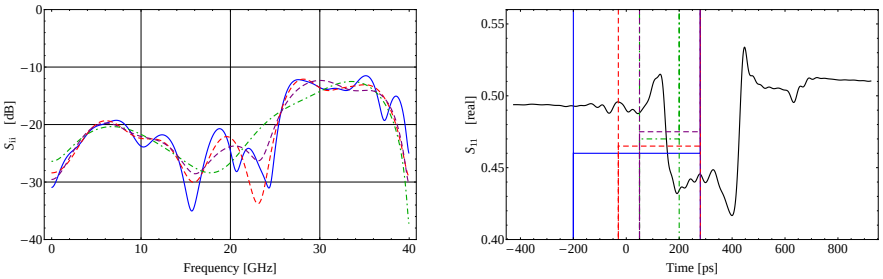

(a) Gated S11 measurements. Gates indicated in Figure 9.7(b).

(b) Time domain measurement.

Figure 9.7: First plug of design G PCB M190410 (short PCB).

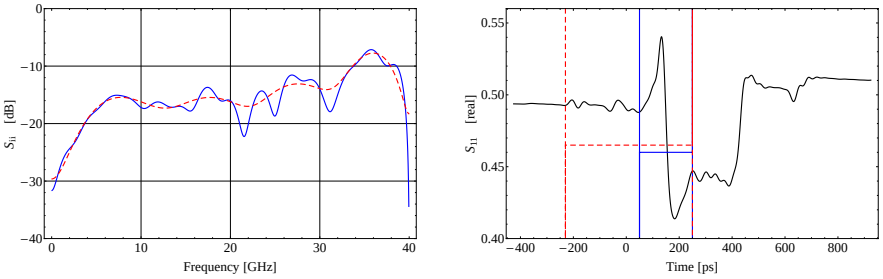

(a) Gated S11 measurements. Gates indicated in Figure 9.8(b).

(b) Time domain measurement.

Figure 9.8: Second plug of design G PCB M190410 (short PCB).

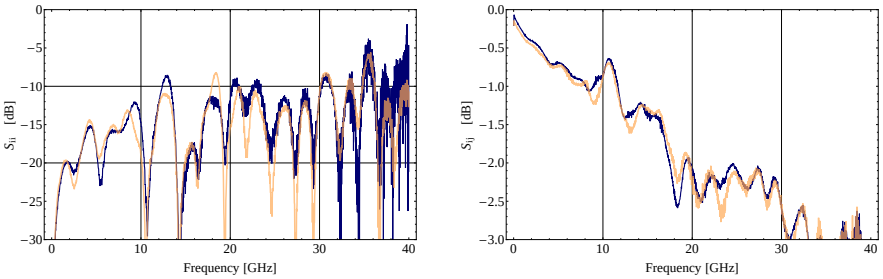

Figure 9.9: The reflectivity and transmission of M190410 without time-gating. Dark blue: S11 respectively S12, light orange: S22 respectively S21.

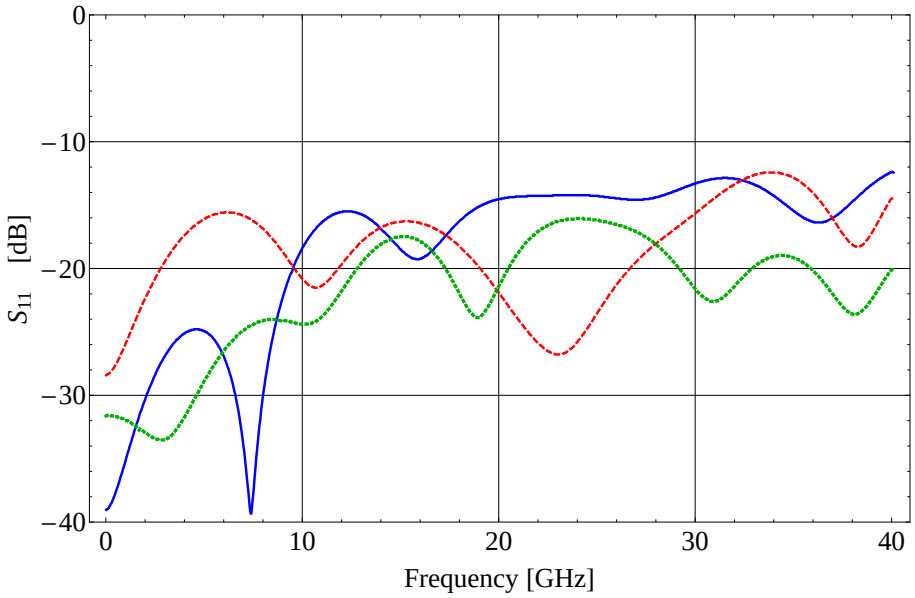

Figure 9.10: The PCBs assembled at Huber and Suhner. S11 of port 1 (blue) and port 2 (red, dashed) of PCB HS1 and port 1 of PCB HS2 (green, dotted). Both samples are straight coplanar waveguides on design E PCB.

connectors there is a gap between the PCB and the connector (as discussed in Section 9.3). The gap of the second connector is larger than the one of the first plug resulting in a higher reflection.

The measured performance of the device is approximately comparable to the simulation results. Figure 9.9 shows the reflectivity and transmission of the PCB without time-gating.

Huber and Suhner, the company which manufactures the plugs, built and tested some PCBs as well. Their test results for HS1 and HS2, PCBs of design E are shown in Figure 9.10

The comparison of the two different lengths of the PCB implies that variations in soldering, which can't fully be prevented, have more influence on the performance of a sample holder than the length of its coplanar waveguide.

The next task was to test a PCB with full metallization on the top layer. The Figures 9.11 to 9.13 show the measurement results of such a device. In general, it is recommended to use ground planes of finite size instead of metallizing the whole top layer. If the whole top layer is metallized, the danger of having resonances caused by standing waves on the top layer is bigger. However, the measurements show no significant increase of reflectivity. Apart from a peak at relatively low frequencies, both, the design G (the short, straight coplanar waveguide) and the design A have a total reflectivity in the order of -10 dB.

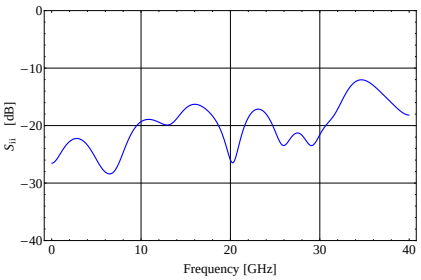

(a) Gated S11 measurements. Gates indicated in Figure 9.11(b).

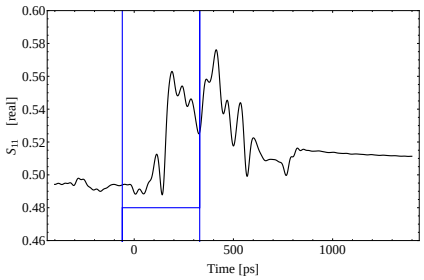

(b) Time domain measurement.

Figure 9.11: First plug of PCB M310510FM with a fully metallized top layer.

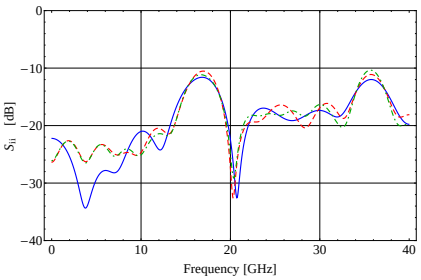

(a) Gated S11 measurements. Gates indicated in Figure 9.12(b).

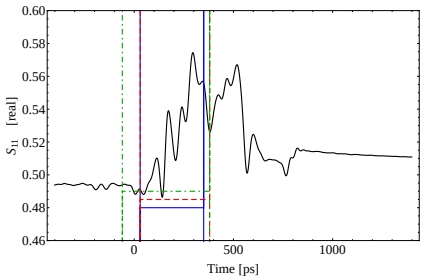

(b) Time domain measurement.

Figure 9.12: Second plug of PCB M310510FM with a fully metallized top layer.

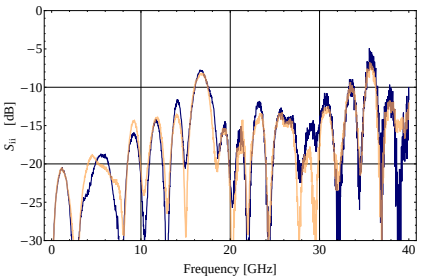

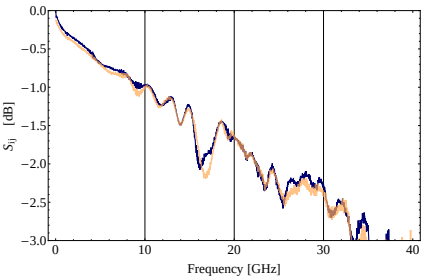

Figure 9.13: The reflectivity and transmission of M310510 without time-gating.Dark blue: S11 respectively S12, light orange: S22 respectively S21.

Chapter 10

Conclusion

Regarding the measurements of straight coplanar waveguides, -10dB of reflectivity is a typical value for the PCB design. Part of the reflectivity might be due to the fact that the impedance of the coplanar waveguide is not exactly 50 Ω. However, most of the reflection is caused by the plugs. In order to have as little reflection as possible at the interface between plugs and board, one has to cut out the residues in the corners of the gap with a scalpel. The performance of the device strongly depends on the quality of the contact between the plug and the board, especially in the region close to the inner conductor. For future designs, one should consider modifying the blueprints in such a way that the gap is slightly enlarged at the corners to ensure that the plug perfectly fits in. Also, the performance of designs featuring curves will be tested in future experiments.

Acknowledgements

I want to thank the whole QuDEV Team for their friendly support. Especially, I would like to thank Prof. Andreas Wallraff for giving me the opportunity to work in a very interesting field of QED.

In particular I want to thank Dr. Stefan Filipp for many constructive discussions and helpful tips.

Furthermore, I am thankful for the possibility to work in this group as a scientific employee.

Bibliography

[1] *Huber+Suhner HF-Verbinder Handbuch*. Huber+Suhner AG, 2007.

[2] Matthias R. Gaberdiel. *Klassische Elektrodynamik*. 2004.

[3] Agilent Technologies Inc. Time domain analysis using a network analyzer. http://cp.literature.agilent.com/litweb/pdf/5989-5723EN.pdf.

[4] D. M. Pozar. *Microwave Engineering, Third Edition*. John Wiley & Sons, Inc., 2005.

[5] R. N. Simons. *Coplanar Waveguide Circuits, Components, and Systems*. John Wiley & Sons, Inc., 1949.